ECM Compliance Regulates Osteogenesis by Influencing MAPK Signaling Downstream of RhoA and ROCK

Chirag B. Khatiwala,[1] Peter D. Kim,[2] Shelly R. Peyton,[1] and Andrew J. Putnam[1,2]

ABSTRACT: The compliance of the extracellular matrix (ECM) regulates osteogenic differentiation by modulating extracellular signal-regulated kinase (ERK) activity. However, the molecular mechanism linking ECM compliance to the ERK-mitogen-activated protein kinase (MAPK) pathway remains unclear. Furthermore, RhoA has been widely implicated in integrin-mediated signaling and mechanotransduction. We studied the relationship between RhoA and ERK-MAPK signaling to determine their roles in the regulation of osteogenesis by ECM compliance. Inhibition of RhoA and ROCK in MC3T3-E1 pre-osteoblasts cultured on substrates of varying compliance reduced ERK activity, whereas constitutively active RhoA enhanced it. The expression of RUNX2, a potent osteogenic transcription factor, was increased on stiffer matrices and correlated with elevated ERK activity. Inhibition of RhoA, ROCK, or the MAPK pathway diminished RUNX2 activity and delayed the onset of osteogenesis as shown by altered osteocalcin (OCN) and bone sialoprotein (BSP) gene expression, alkaline phosphatase (ALP) activity, and matrix mineralization. These data establish that one possible mechanism by which ECM rigidity regulates osteogenic differentiation involves MAPK activation downstream of the RhoA–ROCK signaling pathway.
J Bone Miner Res 2009;24:886–898. Published online on December 29, 2008; doi: 10.1359/JBMR.081240

Address correspondence to: *Andrew J. Putnam, Department of Biomedical Engineering, 3107 Natural Sciences II, University of California, Irvine, CA 92697-2575, USA, E-mail: aputnam@uci.edu*

INTRODUCTION

CELL ADHESION TO the extracellular matrix (ECM) by integrins confers biochemical information about the cellular microenvironment, initiating signaling cascades in a manner similar to other receptor–ligand interactions.[1] After adhesion to the ECM, integrins cluster in the plane of the plasma membrane and activate various protein tyrosine kinases (such as focal adhesion kinase [FAK], Src, and Abl), serine-threonine kinases (such as mitogen-activated protein kinase [MAPK], and protein kinase C), and GTPases of the Rho-family (RhoA, Rac, Cdc42).[2–4] In the past decade, an instructive role for the mechanical properties of the ECM has also been identified. Numerous studies using polyacrylamide substrates with tunable mechanical properties have shown that cell morphology, motility, cytoskeletal assembly, and differentiation of a variety of cells types can be influenced by substrate mechanics.[5–11]

It is widely recognized that mechanical stresses play a critical role in bone development and adaptation, an idea first proposed by Julius Wolff in the late 1800s.[12,13] Wolff's Law, which implies that bone grows and adapts in response to mechanical stresses, has been strengthened by a multitude of studies showing that applied stresses influence bone development and remodeling.[14] Furthermore, recent experimental evidence documenting the sensitivity of a multitude of cell types to mechanical cues, either applied extracellularly or intrinsic to the cellular microenvironment, suggests that Wolff's Law may be a much more general organizing principle.[15] Consistent with this idea, one particularly relevant study showed that matrix elasticity governs the differentiation of mesenchymal stem cells (MSCs) into neurogenic, myogenic, or osteogenic lineages in a manner that depends on non-muscle myosin II motor proteins.[6] These observations support the idea that ECM mechanics modulate myosin-mediated actin contractility in a variety of cell types. However, the molecular mechanisms by which mechanical changes in ECM-integrin-cytoskeletal linkages are transduced into functional changes in gene expression to ultimately determine lineage specification are yet to be determined.

The extracellular signal-regulated kinase (ERK), a member of the MAPK cascade, conveys information about the extracellular environment to the nucleus and plays a critical role in osteoblast differentiation and skeletal development.[16] In addition to its participation in growth factor regulation

[1]Department of Chemical Engineering and Materials Science, The Henry Samueli School of Engineering University of California, Irvine, California, USA; [2]Department of Biomedical Engineering, The Henry Samueli School of Engineering University of California, Irvine, California, USA.

of proliferation and apoptosis, the ERK–MAPK pathway has important functions in differentiation as well.[17–24] It has been implicated in the response of bone to a variety of signals, including hormone/growth factor stimulation,[23,25,26] ECM-integrin binding,[22,27] and mechanical loading.[28] Furthermore, we recently showed that ERK activation is involved in the regulation of osteoblastic differentiation by ECM compliance.[29] However, the molecular pathway linking ECM mechanics to a change in ERK activity remains unknown.

We hypothesized that RhoA might play a critical role linking changes in ECM compliance to changes in cellular phenotype. A member of the larger Rho-family of GTPases, RhoA, has been widely implicated in integrin-mediated signaling[30–32] and in the control of cell migration.[33–35] RhoA plays a critical role in the assembly of actin stress fibers in response to various stimuli,[36–38] mediated in part by one of its downstream effectors, the Rho-associated protein kinase, or ROCK. It has also been implicated in the cellular response to mechanical stress and the maintenance of tensional homeostasis.[39–44] Other studies have shown that RhoA regulates the switch between adipogenesis and myogenesis[45] and that osteogenic commitment also relies on RhoA-ROCK signaling.[46] However, despite numerous inferences for a role for RhoA in mechanotransduction, its ability to transduce a change in ECM compliance to changes in osteogenic differentiation and gene expression has never been proven.

Therefore, we set out to address whether ECM compliance modulates osteogenesis through a RhoA-dependent mechanism and to determine whether a linkage between the RhoA–ROCK and ERK–MAPK pathways is responsible for the control of osteogenic gene expression. To test this hypothesis, MC3T3-E1 pre-osteoblasts were cultured on collagen-functionalized poly(ethylene glycol) (PEG) hydrogels. Much like the widely used polyacrylamide substrates, the PEG hydrogel substrates permit control of the elastic modulus independent of changes in ligand density, as we have previously described.[29,47] However, unlike acrylamide gels, these PEG substrates support long-term cultures without cytotoxicity and are amenable to both 3D cultures and in vivo work. The use of the MC3T3-E1 cell line as a relevant model of lineage commitment was based partly on the fact that the temporal sequence of expressed genes and proteins encoding osteoblast phenotype markers follows the specific pattern of expression observed during fetal calvarial development in vivo.[48] RhoA activity in these pre-osteoblastic cells was manipulated either through the expression of constitutively active RhoA or by the use of C3 toxin. The data described here definitively link ECM compliance, RhoA–ROCK, and ERK–MAPK with the expression of RUNX2, a critical transcription factor in bone development,[49] and thereby provide one possible molecular mechanism by which ECM mechanics regulates osteogenesis.

MATERIALS AND METHODS

Cell culture and reagents

Pre-osteoblastic MC3T3-E1 cells (subclone 4, ATCC), between passages 3 and 9, were maintained and expanded in normal growth medium[29] supplemented with 10 mM β-glycerol phosphate, 50 μg/ml ascorbic acid, and 100 nM dexamethasone (all from Sigma) at 37°C and 5% CO_2. In some experiments, MAPK activation was pharmacologically inhibited using PD98059 (Calbiochem) at a working concentration of 50 μM as previously described.[29] Similarly, ROCK activation was inhibited using Y27632 (Calbiochem) at a working concentration of 10 μM. RhoA activity was inhibited using cell-permeable C3 transferase (C3 toxin; Cytoskeleton, Denver, CO, USA) at a final concentration of 0.5 μg/ml in αMEM culture medium. MC3T3-E1 cells were seeded onto the substrates at identical cell densities (200,000 cells/cm²), and fresh medium with or without drugs was replaced every 2 days for the entire duration of the experiments.

Adenoviral delivery of constitutively active RhoA

To induce MC3T3-E1s to express constitutively active (GTP-bound) RhoA, adenovirus encoding for V14 RhoA-GTP was used as previously described.[50] An appropriate titer was qualitatively determined to be reached when 80–100% of the cells expressed GFP after 48 h of culture. Positive RhoA activity was confirmed by performing a RhoA activation ELISA (RhoA G-LISA Activation Assay; Cytoskeleton) with lysates from transduced and nontransduced cells as per the manufacturer's instructions. RhoA activity was determined spectrophotometrically at 490 nm on a microplate reader (Bio-Rad Laboratories) and normalized to the values obtained from nontransduced cells (arbitrarily assigned a value of 1).

Fabrication and functionalization of poly(ethylene glycol) substrates

PEG hydrogels were prepared by adapting previously published methods.[29,47] Briefly, hydrogels were fabricated by combining 3400-Da PEG-diacrylate (PEGDA), synthesized as described,[50] with nonacrylated PEG (8000 Da; Sigma) to achieve total weight concentrations of 10% or 20%. Substrates of different elastic moduli were generated by varying the relative ratio of cross-linkable PEGDA to inert PEG, with a 50:50 ratio for the soft gels and a 100:0 ratio for the stiff gels. After adding a photoinitiating radical solution (2,2-dimethoxy-2-phenyl-acetophenone in N-vinylpyrrolidinone; both from Sigma; prepared as a 600 mg/ml stock], the gel precursor solution was cast between sterile glass plates separated by 700-μm spacers. Gels were formed by irradiating these solutions with 365-nm UV light for 20 min. Gel discs were punched from the polymerized material using a 0.5-in-diameter steel punch (McMaster-Carr, Atlanta, GA, USA) and placed into multiwell culture plates for subsequent assays. Gels were functionalized to support cell adhesion by covalently attaching type I collagen (Inamed BioMaterials, Fremont, CA, USA) at a theoretical surface density of 50 μg/cm² using a hetero-bifunctional cross-linking agent as previously described.[7] For "rigid" controls, type I collagen was passively adsorbed to the surface of polystyrene dishes as described.[7]

Characterization of PEG hydrogel mechanical properties and type I collagen coupling

Rheological characterization of PEG hydrogels was performed using a Physica MCR301 rheometer (Anton Paar, Ashland, VA, USA) with a parallel-plate geometry and equipped with a peltier unit at 25°C. Two oscillatory tests were completed: an amplitude sweep (strain range of 0.01–100% strain at a fixed frequency of 10 rad/s) and a frequency sweep (frequency range of 0.1–100 rad/s at a fixed strain of 5%). Sandpaper (600 grit) was attached to the parallel plates to prevent slipping of the hydrogel during testing. The complex shear modulus ($G^* = G' + iG''$, where G' is the elastic storage modulus and G'' is the loss modulus) was evaluated using Rheoplus software (Anton Paar). Functionalization of the hydrogel surface with consistent collagen densities independent of gel mechanical or chemical properties was assessed using fluorescent microscopy as previously described.[7] Images taken on an upright Olympus IX51 microscope equipped with a digital camera (Qicam Fast, Qimaging, Surrey, Canada) were quantified using ImageJ software (version1.37; NIH) by evaluating the green channel intensities from multiple images for the same condition. These intensity values were normalized to the values obtained from the images of low collagen density (5 $\mu g/cm^2$) coupled to the soft hydrogels.

Visualization of RUNX2 levels using fluorescence microscopy

At the end of 1, 7, and 14 days, MC3T3-E1 cell nuclei and RUNX2 protein expression levels were visualized using standard fluorescence microscopy. Briefly, cells were fixed using 4% formaldehyde (Sigma) in PBS. Rabbit polyclonal anti-RUNX2 (M-70) IgG (Santa Cruz Biotech) followed by TRITC-conjugated donkey anti-rabbit IgG (Jackson ImmunoResearch) was used to stain for RUNX2. Nuclei were counterstained with DAPI (Sigma). All images were taken on an upright Olympus IX51 microscope equipped with a Qicam Fast digital camera.

Immunoblotting

MAPK activity was assayed after 1 and 14 days as previously described.[29] Briefly, cells were washed in ice-cold PBS and solubilized in MAPK lysis buffer (50 mM Tris, pH 7.5, 0.5 mM EDTA, 50mM NaF, 0.1 M NaCl, 50 mM β-glycerol phosphate, 5 mM sodium pyrophosphate, 1% Triton-X100, and protease inhibitors). Equal protein lysates were subjected to SDS-PAGE, antibody blotting, and sequential membrane reprobing. Blots were probed with antibodies to active MAPK (rabbit monoclonal anti-phospho p44/42 MAPK [Thr 202/ Tyr 204]; Cell Signaling Technology) and β-actin (mouse monoclonal anti-β-actin; Abcam), followed by horseradish peroxidase–conjugated (HRP) IgG antibodies (Santa Cruz Biotech) and an enhanced chemiluminescent substrate. ImageJ was used to obtain densitometric values from developed films, and MAPK activity was determined as a ratio of phosphorylated p44/42 MAPK to β-actin for each condition.

Alkaline phosphatase assay

We measured cellular alkaline phosphatase (ALP) activity, at 1 and 14 days, as previously described.[29] Briefly, cells were washed with cold PBS and lysed using passive lysis buffer (Promega). Lysates were homogenized and subjected to sonication and centrifugation in 10 mM Tris-HCL (pH 7.4; Sigma). ALP activity in the cell lysates was assayed at 37°C in a buffer containing 100 mM glycine and 1 mM $MgCl_2$ (pH 10.5), for 20 min using p-nitrophenol phosphate (50 mM; all from Sigma) as a substrate. The amount of p-nitrophenol liberated was determined spectrophotometrically after the enzymatic reaction was terminated using 0.1 N NaOH. ALP activity (units/ml) was normalized with protein measurements for each sample.

RT-PCR

Total RNA was extracted using the SV Total RNA Isolation kit, and cDNA was synthesized using the ImProm-II reverse transcription kit (both from Promega) as per the manufacturer's instructions. A 2-μl aliquot of the cDNA was used for subsequent PCR amplifications. For each analyzed gene, the primer sequences were the following: bone sialoprotein (accession no. NM_008318) forward, 5′-TGTCTGCTGAAACCCGTTC-3′ and reverse, 5′-GGGGTCTTTAAGTACCGGC-3′, osteocalcin (accession no. NM_001037939) forward, 5′-AGGGA GGATCAAGTCCCG-3′ and reverse, 5′ GAACAGA CTCCGGCGCTA-3′, α1 – type I collagen (accession no. NM_007742) forward, 5′-TTCTCCTGGTAAAGATG GTGC-3′ and reverse, 5′-GGACCAGCATCACCTT TAACA-3′, and internal control GAPDH (accession no. NM_008084) forward, 5′-CCCTGTTGCTGTAGCC GTA-3′ and reverse, 5′-CCGGTGCTGAGTATGTC G-3′. For all genes, the cycling conditions were as follows: denaturing at 94°C for 3 min, amplification by 35 cycles at 94°C (30 s), 56–58°C (30 s), and 72°C (30–45 s), and extension at 72°C for 5 min. Amplified products were resolved by electrophoresis on 2% agarose gels stained with ethidium bromide. Intensities of bands were determined by quantitative densitometry using ImageJ.

Von Kossa staining

MC3T3-E1 cells cultured for 14 days on tissue culture polystyrene were stained for mineral content based on the von Kossa method using a commercial kit (American MasterTech Scientific, Lodi, CA, USA) according to the manufacturer's instructions. Images were taken using a Nikon D80 digital camera.

Statistical analysis

All statistical analyses were performed using InStat 2.01 for Macintosh. Statistical comparisons were made by performing a one-way ANOVA, followed by a Student-Newman-Keuls post-test. $p < 0.05$ denotes statistical significance.

RESULTS

Characterization and functionalization of PEG hydrogels as mechanically tunable substrates

In a prior study using PEG hydrogel substrates with tunable mechanical properties, we showed that ECM compliance regulates the osteogenic differentiation of MC3T3-E1 cells through the MAPK pathway.[29] Because of their tunable biophysical properties, we chose to use these same PEG hydrogels in this study as well. Two sets of substrates were fabricated from polymer solutions in which the amounts of cross-linkable polymer (in this case, PEG-diacrylate or PEGDA; Fig. 1A) were varied, in much the same way that polyacrylamide substrates are fabricated. Photopolymerization of these solutions results in hydrogel formation (Fig. 1B) as previously described.[29] The two sets of substrates used here were chosen based on our earlier study documenting their elastic (i.e., Young's) moduli.[29] The first set of substrates, which we will hereafter refer to as "soft," has an elastic modulus of 13.67 ± 7.07 kPa, whereas the second, hereafter referred to as "stiff," has a value of 423.89 ± 159.43 kPa. In vivo, this range of elasticity is representative of that of striated muscle ($\sim 8-17$ kPa) and that of a mature osteoblastic collagenous bone environment (approximately >100 kPa).[6,51] Rigid polystyrene was used throughout as a control. Our prior studies confirm that the MC3T3-E1 cells exhibit phenotypic changes when cultured on these different substrates. However, to account for the viscoelastic nature of these hydrogels, we performed additional rheological measurements to quantify the complex moduli ($G*$) of these materials. Both frequency sweep and amplitude sweep experiments confirm that the different hydrogels possess mechanical properties that are different by at least an order of magnitude (Fig. 1C).

To render these otherwise protein-resistant substrates amenable for cell adhesion (Fig. 1D), we functionalized the surface of these hydrogels with full-length type I collagen (at a theoretical surface density of 50 $\mu g/cm^2$), an ECM protein that constitutes 85–90% of the organic bone matrix.[52] To confirm that the cells were presented with uniform densities of type I collagen on the surface of the hydrogels, independent of the changes in cross-linking that permit manipulation of the mechanical properties, immunofluorescent staining was used to visually assess the differences between the gels functionalized with either 5- or 50-$\mu g/cm^2$ collagen surface densities. Whereas a distinct, visible increase in collagen density was evident using immunofluorescence staining in the absence of cells on two different substrate stiffnesses (soft and stiff hydrogels), substrates functionalized using solutions with the same starting collagen concentration showed no qualitative difference in collagen immunofluorescence (Fig. 1E). Quantifying these types of images confirmed these qualitative observations (Fig. 1F), showing no significant differences in collagen content across the soft and stiff hydrogels when the same starting amount of collagen is used. Hence, these hydrogels are capable of presenting the cells with uniform ligand densities independent of variations in mechanical properties or polymer chemistries.

Regulation of RhoA activity in MC3T3-E1 cells

Previously we have shown that the cytoskeletal assembly and formation of focal adhesions in MC3T3-E1 cells are regulated by substrate stiffness.[7] It is also known that the activity of the GTP-binding protein RhoA regulates assembly of focal adhesions and stress fibers.[34,53] Furthermore, it was recently shown that matrix elasticity and RhoA activity are independently capable of regulating mesenchymal stem cell lineage commitment.[6,46] Therefore, we molecularly altered RhoA activity using adenoviral constructs encoding for constitutively active (V14-RhoA) or dominant-negative (N19-RhoA) mutants, as well as a potent RhoA inhibitor (C3 toxin; Fig. 2). ELISA detection of GTP-bound RhoA showed that GFP-only–infected cells had RhoA activity identical to uninfected controls, whereas V14-RhoA–infected cells showed a $\sim 50\%$ increase in RhoA activity, and C3 toxin treated cells showed a $\sim 50\%$ decrease. In our hands, the N19-RhoA–infected cells showed only a slight decrease in RhoA activity that was not statistically significant. Therefore, we used cells either infected with V14-RhoA or treated with C3 toxin throughout the remainder of the study. The stability of the adenoviral infections over the entire time course for this study was qualitatively assessed using GFP fluorescence from V14-RhoA–infected cells. No qualitative differences in GFP fluorescence were observed for the entire duration of the study (14 days) from V14-RhoA–infected cells cultured either on the compliant hydrogels or control tissue culture polystyrene substrates (Fig. 2B).

RhoA and ROCK influence the regulation of MAPK activity by ECM compliance

The ERK–MAPK pathway is a major conduit for conveying information about the extracellular environment to changes in gene expression, including changes in substrate compliance.[29] To study the influence of RhoA–ROCK signaling on the regulation of the ERK–MAPK pathway by ECM compliance, it was first confirmed that MAPK phosphorylation varies in MC3T3-E1 cells cultured on substrates of varying rigidity (Fig. 3). After both 1 and 14 days in culture, increased substrate stiffness correlated with enhanced levels of phosphorylated p44/42 MAPK (ERK1/2; Fig. 3). After 1 day, the levels of MAPK activation were not affected by the presence of the various inhibitors or RhoA mutants, regardless of substrate compliance (Figs. 3A and 3B). By day 14, inhibition of RhoA or ROCK (by C3 toxin or Y27632, respectively) significantly reduced MAPK phosphorylation compared with untreated controls (Figs. 3C and 3D). The degree of inhibition was comparable to that induced by the MEK inhibitor PD98059. At this 14-day time point, the expression of V14-RhoA did not significantly alter MAPK activity relative to control, although there was a slight but insignificant increase in MAPK activity evident on the most compliant hydrogels. PD98059 was also still effective as an inhibitor of MAPK activity in the V14-infected cells. Collectively, these data suggest that altering the RhoA–ROCK pathway induces downstream changes in MAPK activity as a function of substrate compliance in MC3T3-E1 cells.
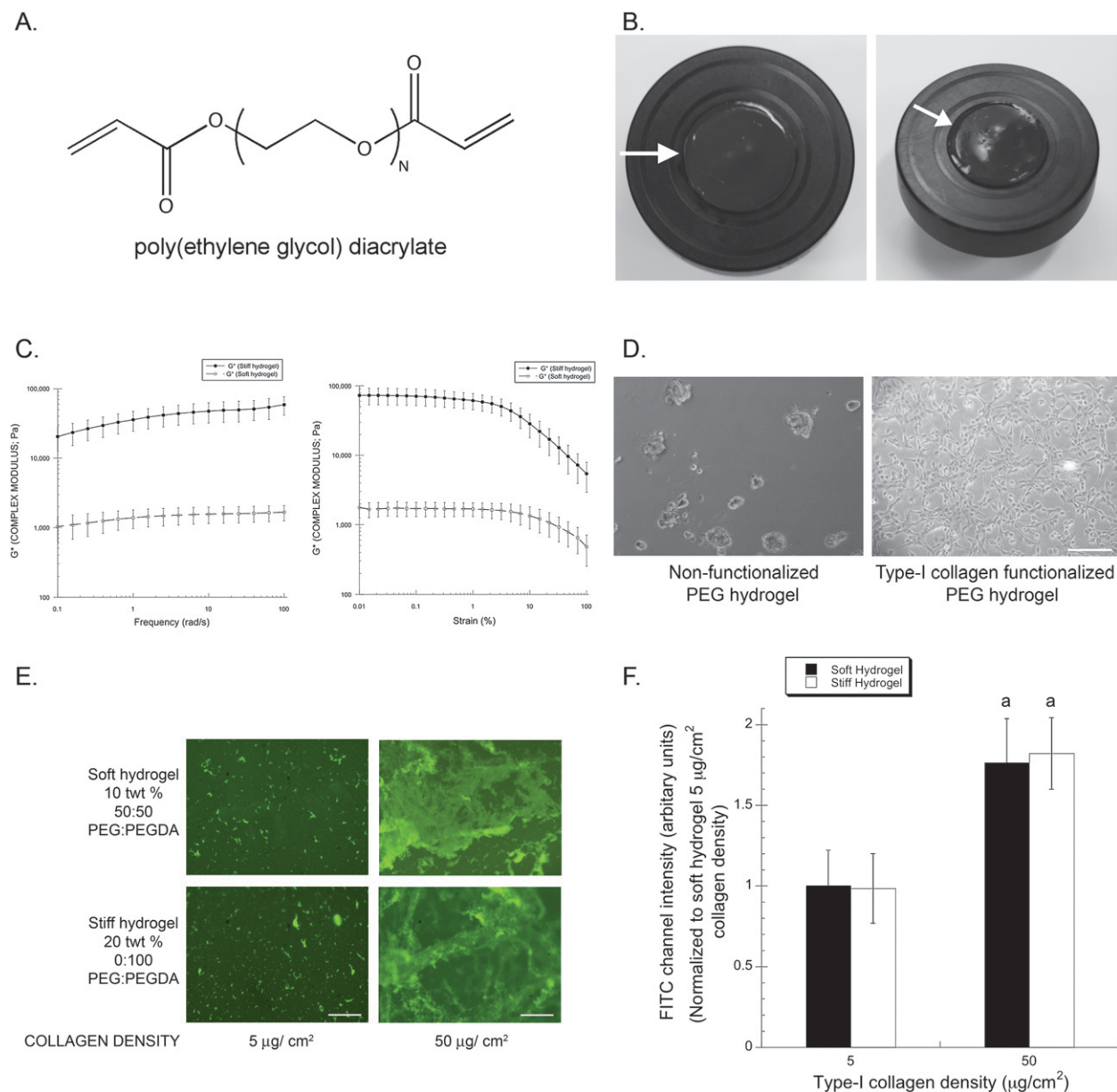
FIG. 1. Mechanical and cell adhesive properties of poly(ethylene glycol) hydrogels are independently tunable. (A) Chemical structure of PEGDA molecule with acrylated end groups responsible for cross-linking. (B) Macroscopic images of a PEG hydrogel (1 in diameter) composed of 10 total polymer weight percent and a 50:50 ratio of PEGDA:PEG (arrow). (C) Complex shear moduli of PEG gels were assessed as a function of strain amplitude (strain sweep) or frequency (frequency sweep). Data represent mean ± SD ($N = 5$). (D) Representative phase contrast images of MC3T3-E1 cells cultured for 12 h on nonfunctionalized (left) and type I collagen functionalized (right) PEG hydrogels are shown (scale bar, 250 μm). (E) Shown are representative immunofluorescent micrographs of PEG hydrogels, composed of either 10 total polymer weight percent and a 50:50 ratio of PEGDA:PEG (top, denoted as soft hydrogel) or 20 total polymer weight percent containing 100% PEGDA (bottom, denoted as stiff hydrogel), coupled with the two different theoretical collagen densities (left: 5 μg/cm²; right: 50 μg/cm²). Scale bar represents 250 μm. (F) Quantification of such images showed a uniform fluorescent intensity for a given concentration irrespective of the substrate stiffness/chemistry. Data represent mean ± SD ($N = 4$; [a]$p < 0.01$ relative to 5 μg/cm² theoretical collagen density intensity levels).

ECM rigidity regulates RUNX2 expression through RhoA, ROCK, and MAPK

RUNX2 is an important transcription factor necessary for osteoblast differentiation and bone formation.[49,54] Of the multiple signaling pathways that converge on RUNX2, MAPK signaling is one of the most prominent.[16,22–24]

However, there is no evidence that ECM compliance and/or RhoA–ROCK pathway influence RUNX2 activity. Here RUNX2 expression was monitored in MC3T3-E1s using immunofluorescence staining (Fig. 4). These data show that ECM rigidity regulates RUNX2 expression levels as early as day 1 (Fig. 4A, top row), with a more pronounced effect after both 7 and 14 days (Figs. 4B and
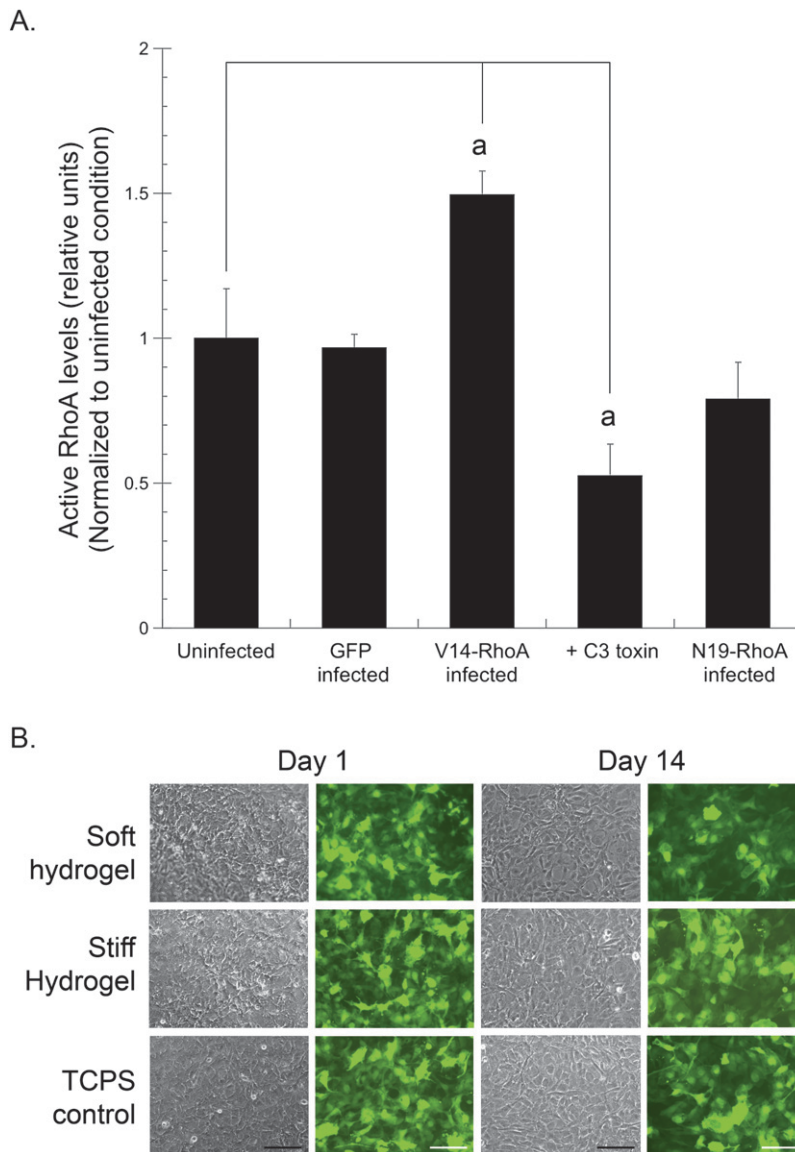
A.

B.

FIG. 2. Altering RhoA activity in MC3T3-E1 cells. (A) MC3T3-E1 cells were adenovirally transduced with vectors encoding for GFP, V14-RhoA, or N19-RhoA or treated with 0.5 µg/ml C3 toxin and cultured on tissue culture polystyrene. After 2 days, active RhoA levels were measured by ELISA. Data represent mean ± SD ($N = 3$; $^a p < 0.001$ relative to control cells). (B) Representative micrographs at 1 and 14 days (phase contrast: columns 1 and 3; fluorescence: columns 2 and 4) of MC3T3-E1 cells expressing V14-RhoA, seeded at confluence on compliant hydrogels and rigid tissue culture polystyrene (TCPS) control (scale bar, 250 µm).

4C, top rows). RUNX2 expression was highest in cells cultured on rigid polystyrene, followed by those on stiff hydrogels. RUNX2 expression was not evident in cells cultured on the soft hydrogels until 14 days. In cells expressing constitutively active V14-RhoA, RUNX2 expression levels were noticeably higher than wildtype cells, especially on the stiff hydrogels after 7 and 14 days (Figs. 4B and 4C, second row). By day 14, even the soft substrates supported elevated RUNX2 levels in the V14-RhoA cells (Fig. 4C). In the case of cells cultured on polystyrene controls, V14-RhoA cells showed high levels of RUNX2 staining comparable to wildtype cells at all time points (Figs. 4A–4C).

Consistent with a mechanistic role for RhoA, C3 toxin dramatically reduced the RUNX2 expression across all substrate conditions and time points. In fact, C3 reduced RUNX2 levels in cells on the stiffer substrates (stiff hydrogels and rigid polystyrene) to levels similar to those on soft hydrogels (Figs. 4A–4C, bottom rows). Downstream of

RhoA, inhibition of ROCK using Y27632 also decreased RUNX2 levels on all substrates at both the 7- and 14-day time points (Figs. 4B and 4C, fourth row). Last, in V14-RhoA–infected cells treated with PD98059, the levels of RUNX2 expression were nearly abolished on all substrates (Figs. 4B and 4C, third row), confirming that MAPK's effects on RUNX2 occur downstream of RhoA signaling in osteoblastic precursor cells.

RhoA–ROCK–MAPK pathway translates changes in ECM compliance to changes in osteogenic gene expression

Osteoblastic differentiation is characterized by increased expression of osteoblast-related genes, such as those encoding for bone sialoprotein (BSP) and osteocalcin (OCN), and ultimately culminates in mineralization of the matrix.[55,56] Our prior work using RGD-functionalized PEG hydrogels showed that the gene expression of BSP and
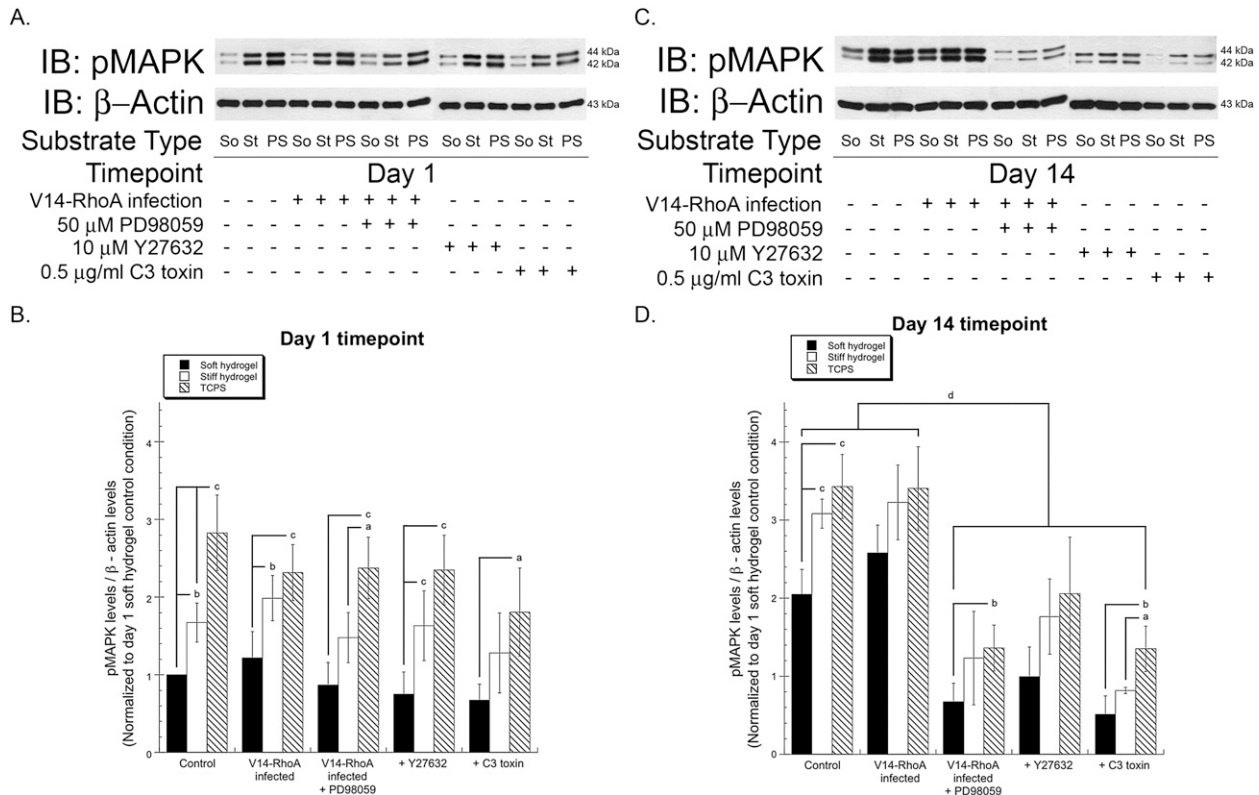
A.

C.

B.

D.

FIG. 3. Inhibition of RhoA or ROCK decreases p44/42 MAPK (ERK1/2) phosphorylation. The levels of phosphorylated p44/42 MAPK (pMAPK) in wildtype and V14-RhoA expressing MC3T3-E1 cells, as a function of substrate stiffness, were detected using standard immunoblotting techniques at day 1 (A) and day 14 (C). β-actin was used as an internal loading control. (So, soft hydrogels; St, stiff hydrogels; PS, control TCPS substrates). Indicated groups were treated with 50 μM PD98059, 10 μM Y27632, or 0.5 μg/ml C3 toxin. (B and D) Quantification was performed using scanning densitometry. The levels of phosphorylated MAPK were normalized to levels of β-actin for each condition at both time points, and the ratios were compared with that of control cells on the soft hydrogel at day 1 (arbitrarily assigned a value of 1). Data represent mean ± SD ($N \geq 3$; [a]$p < 0.05$, [b]$p < 0.01$, and [c]$p < 0.001$ relative to levels on soft hydrogels; [d]$p < 0.01$ relative to wildtype control and V14-RhoA expressing cells).

OCN was regulated by substrate stiffness.[29] Here we used RT-PCR to assess the contributions of the RhoA–ROCK–MAPK pathway on the gene expression levels of BSP, OCN, and type I collagen (α1 chain) as a function of ECM compliance (Fig. 5). After 1 day in culture, BSP gene expression levels correlated with increasing substrate stiffness and were elevated in V14-RhoA cells compared with wildtype controls (Figs. 5A and 5B). Cells treated with C3 toxin, Y27632, and PD98059 expressed similar BSP levels on all substrates. In contrast, OCN (Figs. 5A and 5C) gene expression levels were unchanged across all conditions and on all substrates at this early time point. At day 14, BSP (Figs. 5D and 5E) and OCN (Figs. 5D and 5F) gene expression levels were much higher in both wildtype and V14-RhoA cells compared with those in which MAPK, ROCK, or RhoA activity was inhibited. Furthermore, V14-RhoA–infected cells in which MAPK activation was also inhibited expressed significantly lower expression levels of these osteogenic genes.

Whereas BSP and OCN gene expression levels are elevated during differentiation, expression of type I collagen usually correlates with proliferation of MC3T3-E1 cells and is typically downregulated during the differentiation and mineralization phase in these cells.[48,55,57] In this study, in which confluent cultures were used to separate the effects on proliferation from those on differentiation, we found that altering ECM compliance, RhoA, ROCK, and/or MAPK did not alter the expression of type I collagen gene expression at either of the two time points (Figs. 5A and 5D).

Effects of RhoA, ROCK, and MAPK on ALP activity and matrix mineralization

Increased activity of cellular ALP has frequently been used as an index of osteoblastic differentiation.[58] We have previously shown that ALP activity in MC3T3-E1 cells is regulated by substrate stiffness and MAPK activation.[29] Here we assessed the influence of RhoA, ROCK, and MAPK on ALP activity as a function of substrate compliance (Fig. 6). At day 1, a basal level of ALP activity was observed on all substrates, with no significant differences observed between cells cultured under different conditions on a substrate of a certain compliance (Fig. 6A). However, by day 14, increasing substrate rigidity clearly increased ALP activity, consistent with our prior findings. In addition, cells treated with C3 toxin and Y27632 had significantly lower levels of ALP activity compared with control
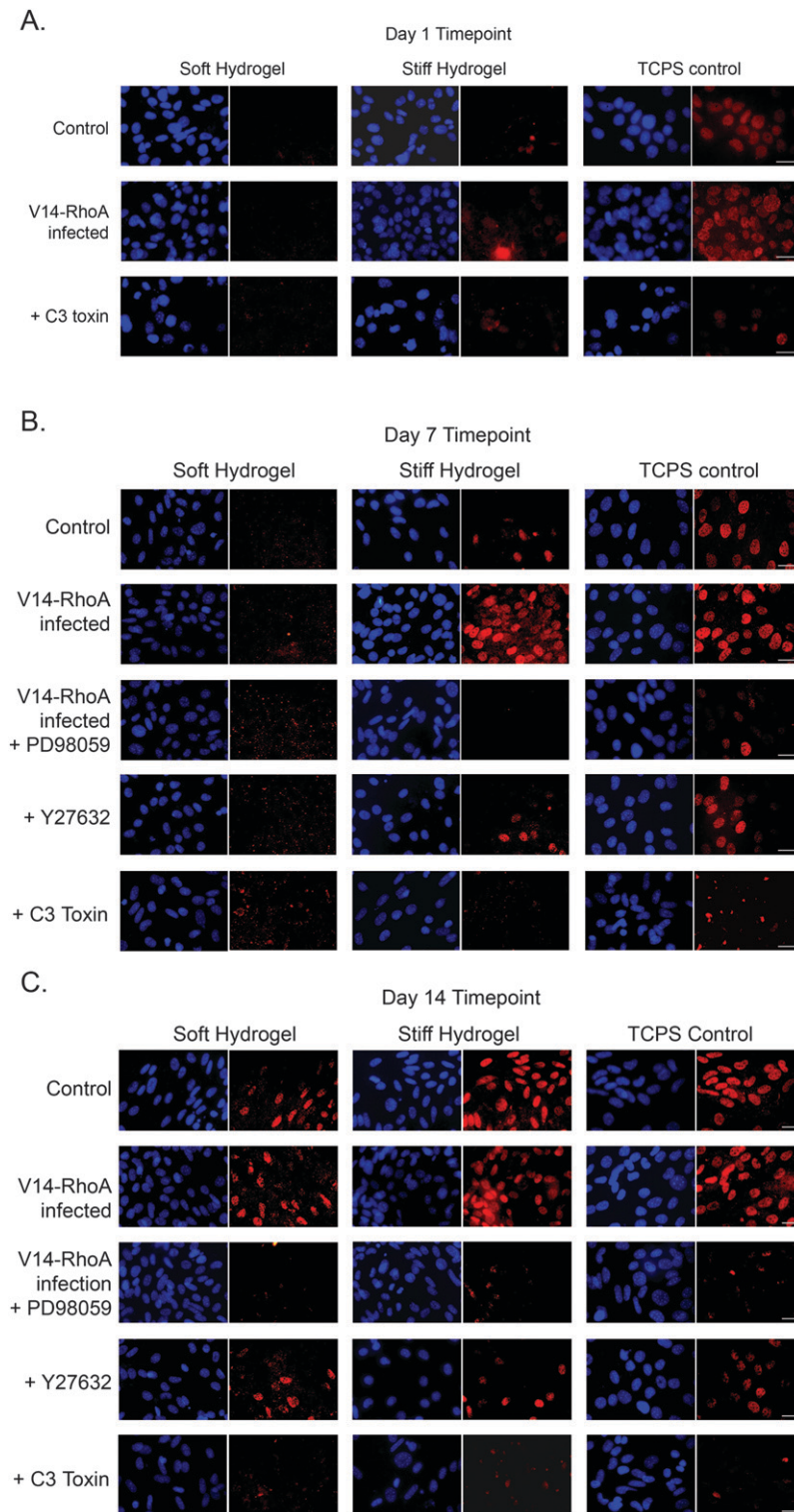
FIG. 4. Matrix rigidity regulates RUNX2 expression in a RhoA-, ROCK-, and MAPK-dependent fashion. RUNX2 protein expression levels were analyzed by immunostaining MC3T3-E1 cells seeded at confluency on compliant hydrogels and rigid polystyrene (TCPS) substrate. Shown are representative immunofluorescent micrographs of MC3T3-E1 cells in which RUNX2 is shown in red, and nuclei are shown in blue (scale bars, 50 μm). (A) After 1 day, RUNX2 expression was evident only in cells cultured on rigid polystyrene (TCPS) but not in cells cultured on hydrogels, and was dependent on level of RhoA activity. (B) MC3T3-E1 cells expressing V14-RhoA showed elevated RUNX2 levels on stiffer matrices (stiff hydrogel and TCPS), whereas cells treated with PD98059, Y27632, or C3 had diminished RUNX2 staining. (C) RUNX2 expression correlated with ECM rigidity in wildtype and V14-RhoA expressing cells, increasing with increasing ECM rigidity. Almost no RUNX2 staining was evident in MC3T3-E1 cells treated with 50 μM PD98059, 10 μM Y27632, or 0.5 μg/ml C3 toxin.

and V14-RhoA cells (Fig. 6B). Furthermore, in V14-RhoA cells treated with PD98059, the levels of ALP activity were significantly lower than in untreated V14-RhoA cells and also relative to untreated wildtype cells. Whereas at this latter time point V14-RhoA–infected cells had higher levels of ALP activity relative to wildtype controls on all sub-

strates, the increase was statistically significant only on the stiff hydrogels.

In the final element of this study, we evaluated the effects of RhoA, ROCK, and MAPK on mineral deposition by MC3T3-E1 cells. Based on our results shown earlier, it was evident that the effects of modulating RhoA, ROCK,
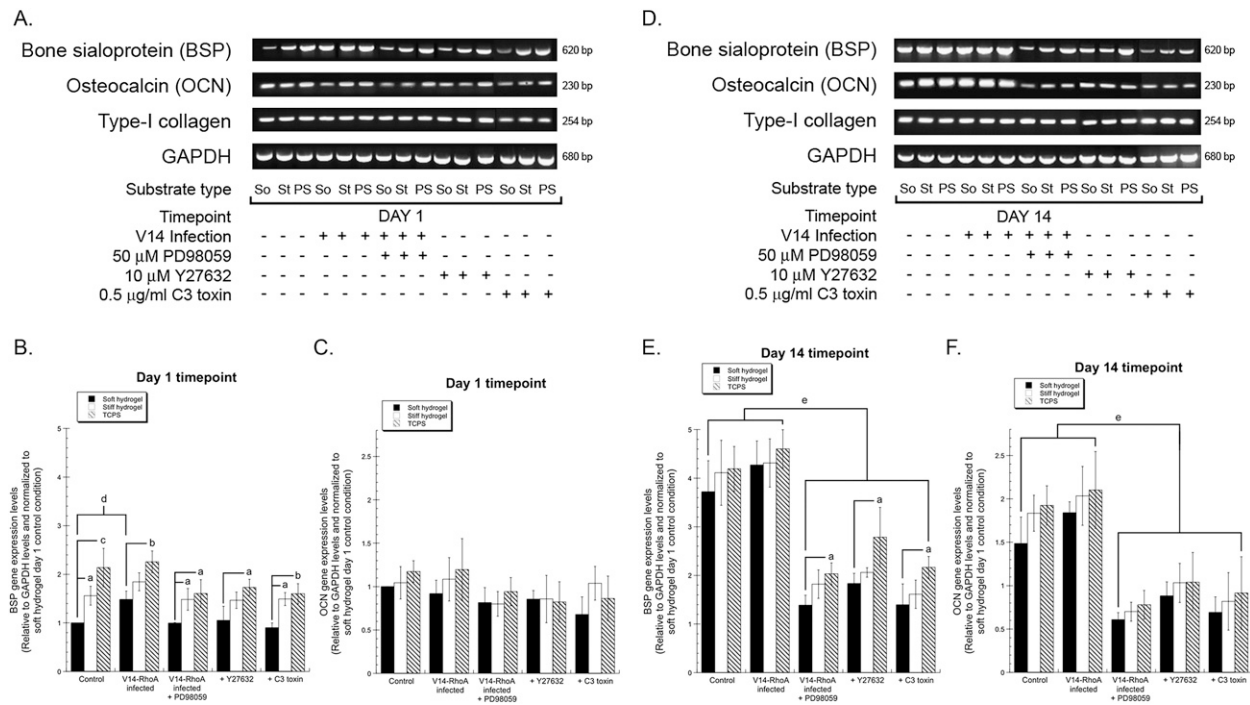
FIG. 5. Altered bone sialoprotein (BSP) and osteocalcin (OCN) gene expression levels in MAPK-, ROCK-, and RhoA-inhibited MC3T3-E1 cells. BSP, OCN, and type I collagen (α1 chain) gene expression levels in wildtype and V14-RhoA expressing MC3T3-E1 cells cultured on the three substrates were assessed by RT-PCR. GAPDH mRNA expression served as an internal control. Representative images of ethidium bromide–stained agarose gels at days 1 (A) and 14 (D) are shown (top panel: BSP, second panel: OCN, third panel: type-I collagen, bottom panel: GAPDH; So, soft hydrogels; St, stiff hydrogels; PS, control polystyrene substrates). Indicated groups were treated with 50 μM PD98059, 10 μM Y27632, or 0.5 μg/ml C3 toxin. Quantification was performed using scanning densitometry. The expression levels of BSP (B and E) and OCN (C and F) were normalized to levels of GAPDH for each condition at both timepoints (B and C: day 1; E and F: day 14), and the ratios were compared with that of wildtype cells on the soft hydrogel at day 1 (arbitrarily assigned a value of 1). Data represent mean ± SD [$N \geq 3$; [a]$p < 0.05$, [b]$p < 0.01$, and [c]$p < 0.001$ relative to levels on soft hydrogels; (B) [d]$p < 0.05$ vs. control cells; (E and F) [e]$p < 0.01$ vs. control wildtype and V14-RhoA expressing cells].

and MAPK inhibition were most pronounced on the stiffest substrate, rigid tissue culture polystyrene. For cells cultured on this substrate, the von Kossa staining method was used to determine the extent of matrix mineralization as an indicator of a mature osteoblast phenotype. After 14 days, we found that both wildtype and V14-RhoA cells deposited densely mineralized matrices, which stain heavily using this technique (Fig. 6C). This is consistent with the hypothesis that osteogenesis is highly efficient on rigid substrates. Furthermore, inhibition of RhoA and ROCK clearly reduced the deposition of mineral as evidenced by a lighter colored and less dense stain. Finally, solidifying our mechanistic understanding of these data, we found that inhibition of the MAPK pathway using PD98059 significantly and clearly reduced mineral deposition by the V14-RhoA cells, supporting the conclusion that RhoA's effects on osteogenesis act through MAPK.

DISCUSSION

In this study, we identified one mechanism by which substrate rigidity regulates osteogenic differentiation. Using type I collagen functionalized substrates spanning an order of magnitude difference in elastic moduli, we found that phosphorylation of ERK, the expression of two osteogenic genes (BSP and OCN), ALP activity, and the de-

position of a mineralized matrix all increased with increasing substrate rigidity. Furthermore, ERK activity was inhibited when either RhoA or ROCK was blocked, whereas cells expressing constitutively active RhoA showed a slight increase in ERK activation on the complaint hydrogels. Inhibition of the RhoA–ROCK pathway blocked the enhanced osteogenic differentiation observed in cells cultured on stiffer matrices. Probing the mechanism further, we also showed that the expression of RUNX2, a transcription factor known to regulate osteogenic differentiation, depends on ECM compliance. RUNX2 levels could be upregulated in cells cultured on compliant hydrogels by expressing constitutively active RhoA and downregulated in cells on all substrates by inhibiting RhoA and ROCK. On the basis of these findings, we propose a model of mechanotransduction by which ECM rigidity regulates osteogenesis through a mechanism involving activation of the MAPK pathway downstream of RhoA and ROCK (Fig. 7).

This proposed mechanosensing mechanism involves integrin cell adhesion receptors, which mediate a reciprocal, bidirectional linkage between cells and the ECM at focal adhesion sites. A number of signaling molecules at and downstream of focal adhesions have been implicated in mechanotransduction,[59] but we hypothesized a role for RhoA because of the fact that it influences both cellular
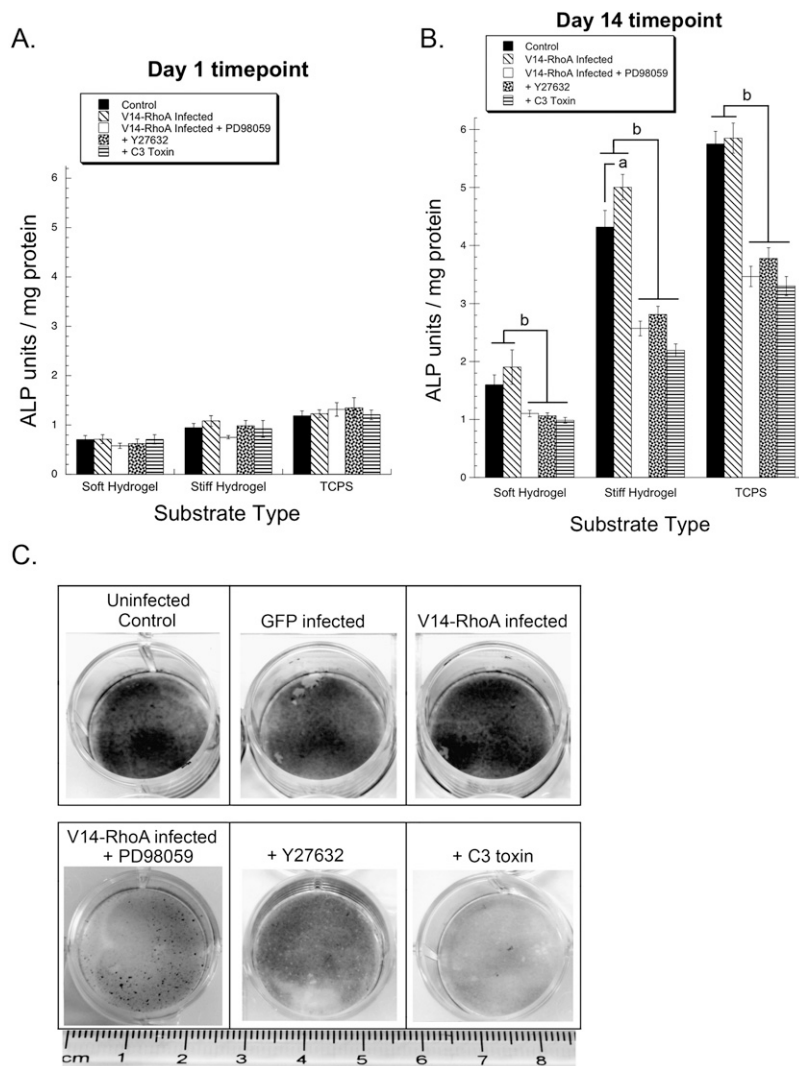
FIG. 6. RhoA, ROCK, and MAPK inhibition decreases ECM compliance–dependent ALP activity and diminishes matrix mineralization. (A and B) Wildtype and V14-RhoA expressing MC3T3-E1 cells were cultured on soft and stiff hydrogels, and control polystyrene (TCPS) either in the absence or presence of 50 μM PD98059, 10 μM Y27632, or 0.5 μg/ml C3 toxin. Cellular ALP activity (normalized by protein concentration) was measured after 1 (A) and 14 (B) days in culture. Data represent mean ± SD ($N \geq 3$; [a]p < 0.05 relative to control wildtype cells; [b]p < 0.001 vs. control wildtype and V14-RhoA expressing cells). (C) MC3T3-E1 cells (wildtype and those adenovirally transduced with vectors encoding for GFP and V14-RhoA) were seeded at confluency in 12-well culture plates and cultured for 14 days either in the absence or presence of 50 μM PD98059, 10 μM Y27632, or 0.5 μg/ml C3 toxin as indicated. Shown are representative images at day 14 of MC3T3-E1 cells fixed and stained using the von Kossa technique for mineralized matrix (dark areas).

biochemistry and biophysics,[34] and repeatedly emerges as a putative mechanosensitive protein. We have also shown in prior work that cells grown on stiff matrices assemble robust actin stress fibers and mature focal adhesions, in contrast to the poorly defined, disorganized F-actin network and small focal adhesions in cells on soft matrices.[7] This clearly suggests RhoA activity increases with increasing ECM rigidity, a conclusion that has been difficult to prove because of both limited sensitivity of RhoA pulldown assays and the inability to fully decouple ECM mechanics from ligand density in most substrate systems. RhoA has also been shown to influence developmental processes.[45,46] McBeath et al.[46] used a micropatterning approach to confine cell shape and showed that MSCs permitted to spread over large adhesive islands adopted an osteogenic fate, whereas those constrained to much smaller adhesive islands adopted an adipogenic fate. The osteogenic fate could be rescued in unspread cells by expressing constitutively active RhoA; likewise, the osteogenic fate could be subverted in spread cells by expressing dominant-negative RhoA. Furthermore, strong recent evidence suggests that ECM compliance can also influence the differentiation of MSCs into an osteoblastic lineage.[6]

However, integrins also stimulate the activation of numerous other signals, often in cooperation with growth factor receptors and their downstream effectors.[2–4] Among the most widely studied of these pathways is that involving the MAPK family, which is known to regulate the proliferation and differentiation of osteoblasts and osteoprogenitor cells.[17–24] In addition, there is convincing evidence that applied mechanical loads stimulate the activation of one or more members of the MAPK family to enhance osteoblast proliferation and differentiation and thereby to increase bone formation.[60–63] Furthermore, it has also been shown that attachment of MC3T3-E1 cells to type I collagen causes phosphorylation of FAK, which in turn activates MAPK, and this signaling cascade is critical for osteoblastic differentiation.[27] We have previously shown that FAK phosphorylation is increased with increasing substrate rigidity in MC3T3-E1 cells (Fig. 7).[7] We have also shown that MAPK activation depends on ECM compliance and is required for osteoblastic differentiation.[29]
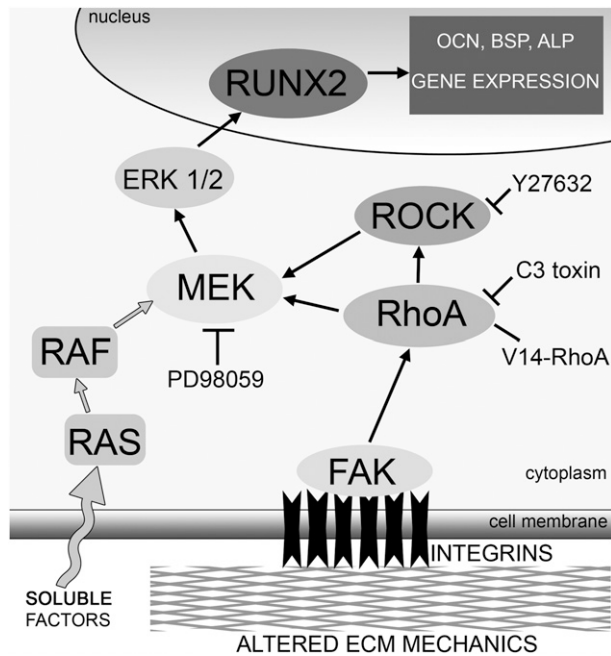
FIG. 7. Model for regulation of osteogenic differentiation of MC3T3-E1 cells by substrate rigidity. In this model, changes in substrate compliance are transduced by integrins (such as $\alpha_2\beta_1$, which binds to type I collagen) that cluster in plane of the plasma membrane, in turn stimulating downstream protein tyrosine kinases such as FAK to catalyze the activations of RhoA. On stiffer matrices, FAK activation is enhanced, leading to higher RhoA activity, thereby promoting increased cellular contractility through ROCK. Cross-talk between RhoA-ROCK and the ERK-MAPK pathway stimulates phosphorylation of ERK 1/2 (p44/42 MAPK) through MEK (MAPK kinase), which regulates the activity of the osteogenic transcription factor RUNX2 to control the expression of osteogenic genes (e.g., OCN and BSP) and ultimately drive differentiation toward a mature osteoblastic phenotype. On softer matrices in the presence of identical soluble cues, however, the diminished activity of FAK, RhoA, and ERK1/2 reduces the levels of RUNX2, inhibiting or at least delaying the subsequent steps of osteogenesis.

Our findings are therefore consistent with prior studies showing the importance of the ERK–MAPK pathway in osteogenesis,[16] the ability of ECM compliance to modulate osteogenesis,[29] and the mechanical sensitivity of the RhoA–ROCK pathway.[64,65] However, until now, these disparate observations had not yet been integrated into a cohesive molecular mechanism linking a change in ECM mechanical properties to a specific transcription factor. To define this mechanism, we transduced MC3T3-E1 cells with adenovirus to express constitutively active RhoA or inhibited RhoA using a cell-permeable C3 toxin. These approaches enabled sustained and significant changes in RhoA activity (~50% increase/decrease) (Fig. 2). We show that whereas these changes in RhoA activity or ROCK inhibition do not alter ERK 1/2 (p44/42 MAPK) phosphorylation at day 1, by day 14 this MAPK activation is significantly reduced when RhoA and ROCK are inhibited (Fig. 3). Treating cells expressing constitutively active RhoA with PD98059, a specific inhibitor of MEK, resulted in significantly lower levels of ERK phosphorylation compared with wildtype cells (Fig. 3). This confirmed that the RhoA–

ROCK pathway effects the classic MAPK pathway (i.e., Ras-Raf-MEK-ERK) at the level of MEK or higher.

Further examining the mechanism by which ECM compliance and RhoA–ROCK signaling regulate osteogenic differentiation, we showed that expression levels of RUNX2, a bone-related transcription factor essential for differentiation of osteoblasts and bone formation,[49] correlate with matrix rigidity as early as day 1 and that inhibition of RhoA and ROCK subvert these even on stiffer matrices (Fig. 4). Prior studies from other investigators have shown that stimulating the ERK–MAPK pathway can activate and phosphorylate RUNX2, a bone-related transcription factor essential for differentiation of osteoblasts and bone formation.[23,24,66,67] Consistent with and extending this known relationship, we found that both RUNX2 expression and ERK activity were highest in cells cultured on the most rigid substrates, with evidence for a correlation as early as day 1. Conversely, despite the presence of identical soluble cues that induce osteogenic differentiation, RUNX2 expression was not detectable in cells cultured on soft substrates until day 14. This correlation between RUNX2 and ECM compliance supports the idea that RUNX2 is mechanosensitive, consistent with two recent studies involving periodontal ligament cells[68] and bone marrow stromal cells.[69] Furthermore, inhibition of either RhoA or ROCK diminished RUNX2 expression, paralleling the effects on ERK phosphorylation even in osteoblastic cells cultured on rigid polystyrene. In addition, in cells expressing constitutively active RhoA and treated with PD98059, little or no RUNX2 expression was observed. Together, these findings suggest that the mechanical cues provided by the ECM are transduced to ERK and RUNX2 downstream of RhoA and ROCK.

Not surprisingly, we found that the expression levels of BSP and OCN (Fig. 5) as well as ALP activity (Fig. 6) was also modulated by ECM compliance and RhoA–ROCK signaling in a MAPK-dependent manner, because RUNX2 is known to directly stimulate their transcription.[49] Finally, perhaps the strongest data we provide linking this RhoA–ROCK and ERK–RUNX2 signaling axis to the regulation of osteogenesis by ECM compliance is provided by our von Kossa matrix mineralization data (Fig. 6C). Even on rigid polystyrene, a substrate that permits maximal levels of ERK activity and RUNX2 expression, inhibition of RhoA and ROCK significantly reduced mineral deposition relative to control cells and to cells expressing constitutively active RhoA.

Whereas our studies presented here focused on ERK and RUNX2 as the primary mediators of RhoA–ROCK signals, other signaling molecules and transcription factors may also participate in this response. Of particular interest, it has been shown that RhoA, through c-*jun* NH$_2$-terminal kinase (JNK), mediates the shear stress–induced activation of transcription factor AP-1[70] and AP-1–related factors like c-*fos*.[71] These transcription factors regulate gene expression by binding to AP-1 sites in osteoblast-related genes and interacting with RUNX2.[66] Whereas MC3T3-E1 cells used in this study were not subjected to any shear stress, the possible involvement of these other transcription factors cannot be ruled out and warrants further study.

In summary, we identified the RhoA–ROCK pathway as an important regulator of osteogenic differentiation that can transduce mechanical cues from the ECM (i.e., changes in matrix elasticity), contributing to a better understanding of the signaling mechanisms responsible for linking changes in ECM compliance to changes in cellular phenotype. Whereas we maintained an identical and constant set of soluble cues in this study, it is also known that various soluble growth factors regulate skeletal development and growth by activating RUNX2 through the MAPK pathway. It will be important in future work to understand how different soluble factors may synergize with ECM compliance to regulate osteogenesis and to determine the role of RhoA-ROCK-ERK–dependent signaling in this synergy.

ACKNOWLEDGMENTS

REFERENCES

1. Hynes RO 1992 Integrins: Versatility, modulation, and signaling in cell adhesion. Cell **69:**11–25.
2. Clark EA, Brugge JS 1995 Integrins and signal transduction pathways: The road taken. Science **268:**233–239.
3. Schwartz MA 1997 Integrins, oncogenes, and anchorage independence. J Cell Biol **139:**575–578.
4. Howe A, Aplin AE, Alahari SK, Juliano RL 1998 Integrin signaling and cell growth control. Curr Opin Cell Biol **10:**220–231.
5. Engler A, Bacakova L, Newman C, Hategan A, Griffin M, Discher D 2004 Substrate compliance versus ligand density in cell on gel responses. Biophys J **86:**617–628.
6. Engler AJ, Sen S, Sweeney HL, Discher DE 2006 Matrix elasticity directs stem cell lineage specification. Cell **126:**677–689.
7. Khatiwala CB, Peyton SR, Putnam AJ 2006 Intrinsic mechanical properties of the extracellular matrix affect the behavior of pre-osteoblastic MC3T3-E1 cells. Am J Physiol Cell Physiol **290:**C1640–C1650.
8. Peyton SR, Putnam AJ 2005 Extracellular matrix rigidity governs smooth muscle cell motility in a biphasic fashion. J Cell Physiol.
9. Polte TR, Eichler GS, Wang N, Ingber DE 2004 Extracellular matrix controls myosin light chain phosphorylation and cell contractility through modulation of cell shape and cytoskeletal prestress. Am J Physiol Cell Physiol **286:**C518–C528.
10. Wong JY, Velasco A, Rajagopalan P, Pham Q 2003 Directed movement of vascular smooth muscle cells on gradient-compliant hydrogels. Langmuir **19:**1908–1913.
11. Pelham RJ Jr, Wang Y 1997 Cell locomotion and focal adhesions are regulated by substrate flexibility. Proc Natl Acad Sci USA **94:**13661–13665.
12. Koch JC 1917 The laws of bone architecture. Am J Anat **21:**177–298.
13. Wolff J 1982 Das Gesetz der Transformation der Knochen. Verlag August Hirschwald, Berlin, Germany.
14. Sikavitsas VI, Temenoff JS, Mikos AG 2001 Biomaterials and bone mechanotransduction. Biomaterials **22:**2581–2593.
15. Peyton SR, Ghajar CM, Khatiwala CB, Putnam AJ 2007 The emergence of ECM mechanics and cytoskeletal tension as important regulators of cell function. Cell Biochem Biophys **47:**300–320.
16. Ge C, Xiao G, Jiang D, Franceschi RT 2007 Critical role of the extracellular signal-regulated kinase-MAPK pathway in osteoblast differentiation and skeletal development. J Cell Biol **176:**709–718.
17. Higuchi C, Myoui A, Hashimoto N, Kuriyama K, Yoshioka K, Yoshikawa H, Itoh K 2002 Continuous inhibition of MAPK signaling promotes the early osteoblastic differentiation and mineralization of the extracellular matrix. J Bone Miner Res **17:**1785–1794.
18. Jadlowiec J, Koch H, Zhang X, Campbell PG, Seyedain M, Sfeir C 2004 Phosphophoryn regulates the gene expression and differentiation of NIH3T3, MC3T3-E1, and human mesenchymal stem cells via the integrin/MAPK signaling pathway. J Biol Chem **279:**53323–53330.
19. Jaiswal RK, Jaiswal N, Bruder SP, Mbalaviele G, Marshak DR, Pittenger MF 2000 Adult human mesenchymal stem cell differentiation to the osteogenic or adipogenic lineage is regulated by mitogen-activated protein kinase. J Biol Chem **275:**9645–9652.
20. Klees RF, Salasznyk RM, Kingsley K, Williams WA, Boskey A, Plopper GE 2005 Laminin-5 induces osteogenic gene expression in human mesenchymal stem cells through an ERK-dependent pathway. Mol Biol Cell **16:**881–890.
21. Salasznyk RM, Klees RF, Hughlock MK, Plopper GE 2004 ERK signaling pathways regulate the osteogenic differentiation of human mesenchymal stem cells on collagen I and vitronectin. Cell Commun Adhes **11:**137–153.
22. Xiao G, Gopalakrishnan R, Jiang D, Reith E, Benson MD, Franceschi RT 2002 Bone morphogenetic proteins, extracellular matrix, and mitogen-activated protein kinase signaling pathways are required for osteoblast-specific gene expression and differentiation in MC3T3-E1 cells. J Bone Miner Res **17:**101–110.
23. Xiao G, Jiang D, Gopalakrishnan R, Franceschi RT 2002 Fibroblast growth factor 2 induction of the osteocalcin gene requires MAPK activity and phosphorylation of the osteoblast transcription factor, Cbfa1/Runx2. J Biol Chem **277:**36181–36187.
24. Xiao G, Jiang D, Thomas P, Benson MD, Guan K, Karsenty G, Franceschi RT 2000 MAPK pathways activate and phosphorylate the osteoblast-specific transcription factor, Cbfa1. J Biol Chem **275:**4453–4459.
25. Chen C, Koh AJ, Datta NS, Zhang J, Keller ET, Xiao G, Franceschi RT, D'Silva NJ, McCauley LK 2004 Impact of the mitogen-activated protein kinase pathway on parathyroid hormone-related protein actions in osteoblasts. J Biol Chem **279:**29121–29129.
26. Hurley MM, Marcello K, Abreu C, Kessler M 1996 Signal transduction by basic fibroblast growth factor in rat osteoblastic Py1a cells. J Bone Miner Res **11:**1256–1263.
27. Takeuchi Y, Suzawa M, Kikuchi T, Nishida E, Fujita T, Matsumoto T 1997 Differentiation and transforming growth factor-betareceptor down-regulation by collagen-alpha2beta1 integrin interaction is mediated by focal adhesion kinase and its downstream signals in murine osteoblastic cells. J Biol Chem **272:**29309–29316.
28. You J, Reilly GC, Zhen X, Yellowley CE, Chen Q, Donahue HJ, Jacobs CR 2001 Osteopontin gene regulation by oscillatory fluid flow via intracellular calcium mobilization and activation of mitogen-activated protein kinase in MC3T3-E1 osteoblasts. J Biol Chem **276:**13365–13371.
29. Khatiwala CB, Peyton SR, Metzke M, Putnam AJ 2007 The regulation of osteogenesis by ECM rigidity in MC3T3-E1 cells requires MAPK activation. J Cell Physiol **211:**661–672.
30. Ren XD, Kiosses WB, Schwartz MA 1999 Regulation of the small GTP-binding protein Rho by cell adhesion and the cytoskeleton. EMBO J **18:**578–585.

31. Schoenwaelder SM, Burridge K 1999 Bidirectional signaling between the cytoskeleton and integrins. Curr Opin Cell Biol **11:**274–286.

32. Clark EA, King WG, Brugge JS, Symons M, Hynes RO 1998 Integrin-mediated signals regulated by members of the rho family of GTPases. J Cell Biol **142:**573–586.

33. Etienne-Manneville S, Hall A 2002 Rho GTPases in cell biology. Nature **420:**629–635.

34. Hall A 1998 Rho GTPases and the actin cytoskeleton. Science **279:**509–514.

35. Wittmann T, Waterman-Storer CM 2001 Cell motility: Can Rho GTPases and microtubules point the way? J Cell Sci **114:**3795–3803.

36. Chong LD, Traynor-Kaplan A, Bokoch GM, Schwartz MA 1994 The small GTP-binding protein Rho regulates a phosphatidylinositol 4- phosphate 5-kinase in mammalian cells. Cell **79:**507–513.

37. Chrzanowska-Wodnicka M, Burridge K 1996 Rho-stimulated contractility drives the formation of stress fibers and focal adhesions. J Cell Biol **133:**1403–1415.

38. Nobes CD, Hall A 1995 Rho, rac, and cdc42 GTPases regulate the assembly of multimolecular focal complexes associated with actin stress fibers, lamellipodia, and filopodia. Cell **81:**53–62.

39. Putnam AJ, Cunningham JJ, Pillemer BB, Mooney DJ 2003 External mechanical strain regulates membrane targeting of Rho GTPases by controlling microtubule assembly. Am J Physiol Cell Physiol **284:**C627–C639.

40. Matthews BD, Overby DR, Mannix R, Ingber DE 2006 Cellular adaptation to mechanical stress: Role of integrins, Rho, cytoskeletal tension and mechanosensitive ion channels. J Cell Sci **119:**508–518.

41. Aikawa R, Komuro I, Yamazaki T, Zou Y, Kudoh S, Zhu W, Kadowaki T, Yazaki Y 1999 Rho family small G proteins play critical roles in mechanical stress-induced hypertrophic responses in cardiac myocytes. Circ Res **84:**458–466.

42. Aoki H, Izumo S, Sadoshima J 1998 Angiotensin II activates RhoA in cardiac myocytes: A critical role of RhoA in angiotensin II-induced premyofibril formation. Circ Res **82:**666–676.

43. Katsumi A, Milanini J, Kiosses WB, del Pozo MA, Kaunas R, Chien S, Hahn KM, Schwartz MA 2002 Effects of cell tension on the small GTPase Rac. J Cell Biol **158:**153–164.

44. Numaguchi K, Eguchi S, Yamakawa T, Motley ED, Inagami T 1999 Mechanotransduction of rat aortic vascular smooth muscle cells requires RhoA and intact actin filaments. Circ Res **85:**5–11.

45. Sordella R, Jiang W, Chen GC, Curto M, Settleman J 2003 Modulation of Rho GTPase signaling regulates a switch between adipogenesis and myogenesis. Cell **113:**147–158.

46. McBeath R, Pirone DM, Nelson CM, Bhadriraju K, Chen CS 2004 Cell shape, cytoskeletal tension, and RhoA regulate stem cell lineage commitment. Dev Cell **6:**483–495.

47. Peyton SR, Raub CB, Keschrumrus VP, Putnam AJ 2006 The use of poly(ethylene glycol) hydrogels to investigate the impact of ECM chemistry and mechanics on smooth muscle cells. Biomaterials **27:**4881–4893.

48. Raouf A, Seth A 2000 Ets transcription factors and targets in osteogenesis. Oncogene **19:**6455–6463.

49. Ducy P 2000 Cbfa1: A molecular switch in osteoblast biology. Dev Dyn **219:**461–471.

50. Peyton SR, Kim PD, Ghajar CM, Seliktar D, Putnam AJ 2008 The effects of matrix stiffness and RhoA on the phenotypic plasticity of smooth muscle cells in a 3-D biosynthetic hydrogel system. Biomaterials **29:**2597–2607.

51. Engler AJ, Griffin MA, Sen S, Bonnemann CG, Sweeney HL, Discher DE 2004 Myotubes differentiate optimally on substrates with tissue-like stiffness: Pathological implications for soft or stiff microenvironments. J Cell Biol **166:**877–887.

52. Aubin JE, Liu F, Malaval L, Gupta AK 1995 Osteoblast and chondroblast differentiation. Bone **17**(Suppl):77S–83S.

53. Ridley AJ, Hall A 1992 The small GTP-binding protein rho regulates the assembly of focal adhesions and actin stress fibers in response to growth factors. Cell **70:**389–399.

54. Komori T, Yagi H, Nomura S, Yamaguchi A, Sasaki K, Deguchi K, Shimizu Y, Bronson RT, Gao YH, Inada M, Sato M, Okamoto R, Kitamura Y, Yoshiki S, Kishimoto T 1997 Targeted disruption of Cbfa1 results in a complete lack of bone formation owing to maturational arrest of osteoblasts. Cell **89:**755–764.

55. Choi JY, Lee BH, Song KB, Park RW, Kim IS, Sohn KY, Jo JS, Ryoo HM 1996 Expression patterns of bone-related proteins during osteoblastic differentiation in MC3T3-E1 cells. J Cell Biochem **61:**609–618.

56. Franceschi RT 1999 The developmental control of osteoblast-specific gene expression: Role of specific transcription factors and the extracellular matrix environment. Crit Rev Oral Biol Med **10:**40–57.

57. Aubin JE 1998 Advances in the osteoblast lineage. Biochem Cell Biol **76:**899–910.

58. Farley JR, Baylink DJ 1986 Skeletal alkaline phosphatase activity as a bone formation index in vitro. Metabolism **35:**563–571.

59. Bershadsky AD, Balaban NQ, Geiger B 2003 Adhesion-dependent cell mechanosensitivity. Annu Rev Cell Dev Biol **19:**677–695.

60. Kapur S, Baylink DJ, Lau KH 2003 Fluid flow shear stress stimulates human osteoblast proliferation and differentiation through multiple interacting and competing signal transduction pathways. Bone **32:**241–251.

61. Reusch HP, Chan G, Ives HE, Nemenoff RA 1997 Activation of JNK/SAPK and ERK by mechanical strain in vascular smooth muscle cells depends on extracellular matrix composition. Biochem Biophys Res Commun **237:**239–244.

62. Tseng H, Peterson TE, Berk BC 1995 Fluid shear stress stimulates mitogen-activated protein kinase in endothelial cells. Circ Res **77:**869–878.

63. Wadhwa S, Godwin SL, Peterson DR, Epstein MA, Raisz LG, Pilbeam CC 2002 Fluid flow induction of cyclo-oxygenase 2 gene expression in osteoblasts is dependent on an extracellular signal-regulated kinase signaling pathway. J Bone Miner Res **17:**266–274.

64. Smith PG, Roy C, Zhang YN, Chauduri S 2003 Mechanical stress increases RhoA activation in airway smooth muscle cells. Am J Respir Cell Mol Biol **28:**436–442.

65. Wesselman JP, Kuijs R, Hermans JJ, Janssen GM, Fazzi GE, van Essen H, Evelo CT, Struijker-Boudier HA, De Mey JG 2004 Role of the Rhoa/Rho kinase system in flow-related remodeling of rat mesenteric small arteries in vivo. J Vasc Res **41:**277–290.

66. Franceschi RT, Xiao G 2003 Regulation of the osteoblast-specific transcription factor, Runx2: Responsiveness to multiple signal transduction pathways. J Cell Biochem **88:**446–454.

67. Franceschi RT, Xiao G, Jiang D, Gopalakrishnan R, Yang S, Reith E 2003 Multiple signaling pathways converge on the Cbfa1/Runx2 transcription factor to regulate osteoblast differentiation. Connect Tissue Res **44**(Suppl 1):109–116.

68. Ziros PG, Gil AP, Georgakopoulos T, Habeos I, Kletsas D, Basdra EK, Papavassiliou AG 2002 The bone-specific transcriptional regulator Cbfa1 is a target of mechanical signals in osteoblastic cells. J Biol Chem **277:**23934–23941.

69. Wang FS, Wang CJ, Sheen-Chen SM, Kuo YR, Chen RF, Yang KD 2002 Superoxide mediates shock wave induction of ERK-dependent osteogenic transcription factor (CBFA1) and mesenchymal cell differentiation toward osteoprogenitors. J Biol Chem **277:**10931–10937.

70. Li S, Chen BP, Azuma N, Hu YL, Wu SZ, Sumpio BE, Shyy JY, Chien S 1999 Distinct roles for the small GTPases Cdc42 and Rho in endothelial responses to shear stress. J Clin Invest **103:**1141–1150.

71. Shiu YT, Li S, Yuan S, Wang Y, Nguyen P, Chien S 2003 Shear stress-induced c-fos activation is mediated by Rho in a calcium-dependent manner. Biochem Biophys Res Commun **303:**548–555.